available at www.sciencedirect.com
journal homepage: www.europeanurology.com

European Association of Urology

Prostate Cancer

A Prospective, Blinded Comparison of Magnetic Resonance (MR) Imaging–Ultrasound Fusion and Visual Estimation in the Performance of MR-targeted Prostate Biopsy: The PROFUS Trial

James S. Wysock[a], *Andrew B. Rosenkrantz*[b], *William C. Huang*[a], *Michael D. Stifelman*[a], *Herbert Lepor*[a], *Fang-Ming Deng*[c], *Jonathan Melamed*[c], *Samir S. Taneja*[a,*]

[a] *Division of Urologic Oncology, Department of Urology, New York University Langone Medical Center, New York, NY, USA;* [b] *Department of Radiology, New York University Langone Medical Center, New York, NY, USA;* [c] *Department of Pathology, New York University Langone Medical Center, New York, NY, USA*

Article info

Article history:
Accepted October 30, 2013
Published online ahead of print on November 8, 2013

Keywords:
Magnetic resonance imaging
Prostate biopsy
Prostate cancer
Targeted biopsy

Abstract

Background: Increasing evidence supports the use of magnetic resonance (MR)–targeted prostate biopsy. The optimal method for such biopsy remains undefined, however.
Objective: To prospectively compare targeted biopsy outcomes between MR imaging (MRI)–ultrasound fusion and visual targeting.
Design, setting, and participants: From June 2012 to March 2013, prospective targeted biopsy was performed in 125 consecutive men with suspicious regions identified on prebiopsy 3-T MRI consisting of T2-weighted, diffusion-weighted, and dynamic-contrast enhanced sequences.
Intervention: Two MRI–ultrasound fusion targeted cores per target were performed by one operator using the ei-Nav|Artemis system. Targets were then blinded, and a second operator took two visually targeted cores and a 12-core biopsy.
Outcome measurements and statistical analysis: Biopsy information yield was compared between targeting techniques and to 12-core biopsy. Results were analyzed using the McNemar test. Multivariate analysis was performed using binomial logistic regression.
Results and limitations: Among 172 targets, fusion biopsy detected 55 (32.0%) cancers and 35 (20.3%) Gleason sum $\geq$7 cancers compared with 46 (26.7%) and 26 (15.1%), respectively, using visual targeting ($p = 0.1374$, $p = 0.0523$). Fusion biopsy provided informative nonbenign histology in 77 targets compared with 60 by visual ($p = 0.0104$). Targeted biopsy detected 75.0% of all clinically significant cancers and 86.4% of Gleason sum $\geq$7 cancers detected on standard biopsy. On multivariate analysis, fusion performed best among smaller targets. The study is limited by lack of comparison with whole-gland specimens and sample size. Furthermore, cancer detection on visual targeting is likely higher than in community settings, where experience with this technique may be limited.
Conclusions: Fusion biopsy was more often histologically informative than visual targeting but did not increase cancer detection. A trend toward increased detection with fusion biopsy was observed across all study subsets, suggesting a need for a larger study size. Fusion targeting improved accuracy for smaller lesions. Its use may reduce the learning curve necessary for visual targeting and improve community adoption of MR-targeted biopsy.

* Corresponding author. NYU Urology Associates, 150 E 32nd St, 2nd Floor, New York, NY, USA.
Tel. +1 646 825 6300; Fax: +1 646 825 6368.
E-mail address: samir.taneja@nyumc.org (S.S. Taneja).

0302-2838/$ – see back matter
http://dx.doi.org/10.1016/j.eururo.2013.10.048

1. Introduction

Although increasing evidence supports use of multiparametric magnetic resonance imaging (mpMRI)-targeted biopsy (MR-TB) in clinical practice, the optimal methodology for targeting magnetic resonance imaging (MRI)-suspicious regions (mSR) remains unknown [1–6]. In-gantry prostate biopsy of mSR using real-time magnetic resonance (MR) guidance has been reported to have excellent outcomes, but the technique remains restricted to a few centers and is limited by multiple challenges, including a steep learning curve, time investment and the opportunity cost of magnet time [7–11]. Many investigators have used a visual, or cognitive, guidance technique in which the surgeon samples a visually estimated location on ultrasound that corresponds to the mSR location (VE-TB) [12–14]. The accuracy of MR-TB is influenced by multiple variables, including mSR size, alignment of prostate landmarks, and operator experience [15].

Software-based coregistration of MRI–ultrasound (MRI-US) targeted biopsy (MRF-TB) requires demarcation of mSR on prebiopsy MR images and software "fusion" of these images during real-time ultrasound imaging. Several MRF-TB platforms exist, but their accuracy compared with VE-TB remains unclear. Consequently, we undertook a prospective, blinded comparison of MRF-TB and VE-TB among men undergoing prostate biopsy.

2. Materials and methods

2.1. Study design and population

After receiving institutional review board approval, enrollment began on June 18, 2012, and closed on March 19, 2013. Consecutive men presenting for prostate biopsy underwent prebiopsy mpMRI and were offered inclusion on identification of any mSR. If included, all patients underwent informed consent. Over this period, 210 men presented for prostate biopsy, and 193 (91.9%) underwent mpMRI. Seventeen men (8.1%) were excluded because of MRI contraindications. Prebiopsy mpMRI demonstrated no abnormalities in 32 patients (16.6% of mpMRI), and 45 patients (21.4%) refused inclusion or were excluded (Fig. 1). In total, 125 patients (65.8% of mpMRI) made up the final cohort.

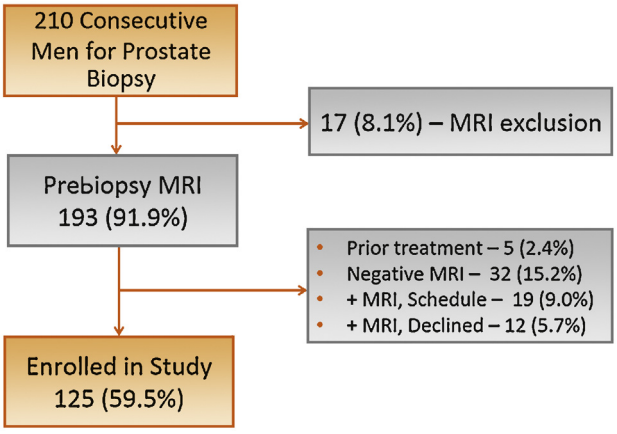

Fig. 1 – Study flow diagram.
MRI = magnetic resonance imaging.

2.2. Multiparametric magnetic resonance imaging protocol

Imaging was performed on a 3-T clinical system (Magnetom Trio, Siemens Healthcare, Erlangen, Germany) using a pelvic phased-array coil. Examinations included multiplanar turbo spin-echo T2-weighted images (T2WI), axial turbo spin-echo T1-weighted images, axial single-shot echo-planar diffusion-weighted imaging, and dynamic contrast-enhanced (DCE) MRI using a three-dimensional (3D) fat-suppressed spoiled gradient-echo T1-weighted sequence. The DCE images were postprocessed using software (Invivo, Schwerin, Germany) that applied a biexponential semiquantitative model to generate parametric maps representing the maximum slope of enhancement and washout of contrast following enhancement peak.

2.3. Multiparametric magnetic resonance imaging interpretation and MRI-suspicious regions demarcation

A single fellowship-trained radiologist who had expertise in prostate imaging evaluated all MRI images according to consensus guidelines for interpretation and reporting of prostate MRI [16]. Examinations with no mSR received a score of 1. For each identified mSR, a score from 2 to 5 was given to stratify suspicion for tumor. The radiologist generated a standardized report that included key images depicting the location, boundaries, maximal diameter, and cross-sectional area for each mSR. This report was used for visual guidance at the time of biopsy.

2.4. Magnetic resonance imaging–ultrasound fusion preparation

Segmentation of two-dimensional (2D) mpMRI images was performed using ProFuse software (Eigen, Grass Valley, CA, USA) to create a 3D MRI map prior to prostate biopsy. Target mSR locations were demarcated in axial T2WI. Maps were exported to portable media for use during prostate biopsy.

Biopsies were performed in left lateral decubitus position using the Pro Focus ultrasound system (BK Medical, Peabody, MA, USA) guided by the ei-Nav|Artemis (Eigen) system, endfire probe, reusable biopsy gun, 18G needles, and local anesthesia with 1% lidocaine infiltration.

The MRF was initiated with a 360° reference scan of 2D ultrasound images. Segmentation of 2D ultrasound generated a 3D virtual ultrasound map. This map was automatically rigidly aligned to 3D MRI maps in three axes followed by manual refinement, as necessary. The segmented MRI and ultrasound surfaces were then nonlinearly (nonrigidly) warped followed by elastic deformation [17]. Demarcated mSR were then marked on the 3D map, and "fusion" of ultrasound and MR images was completed. A 12-point standard biopsy template generated by the Artemis

Please cite this article in press as: Wysock JS, et al. A Prospective, Blinded Comparison of Magnetic Resonance (MR) Imaging–Ultrasound Fusion and Visual Estimation in the Performance of MR-targeted Prostate Biopsy: The PROFUS Trial. Eur Urol (2014), http://dx.doi.org/10.1016/j.eururo.2013.10.048

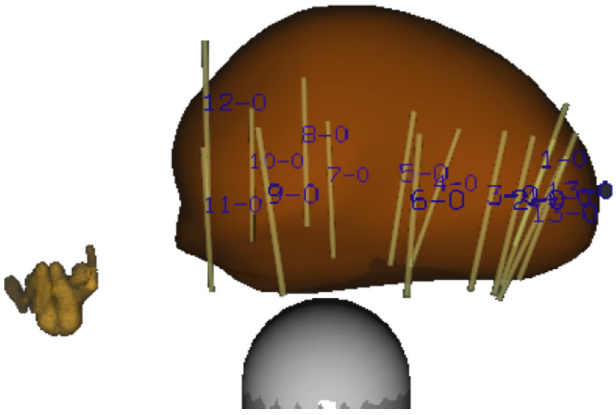

Fig. 2 – Three-dimensional prostate surface map with 12-core biopsy plan.

software was overlaid on the virtual 3D map (Fig. 2). The device was then set to "biopsy" mode, enabling ultrasound probe tracking and projecting biopsy needle trajectories.

A maximum of two mSR per patient were targeted with two cores each by MRF-TB and VE-TB. A single urologist performed all MRF-TB procedures. The location of mSR and MRF-TB were then blinded prior to the entry of the second urologist performing the VE-TB and standard biopsy (Fig. 3).

2.5. Study design and statistical analysis

A study of 125 men was designed to demonstrate a 15% increase in cancer detection rate (CDR) by MRF-TB compared with VE-TB (two-sided $\alpha = 0.05$, $\beta = 0.20$). This sample size was based on institutional experience of a 25% false-negative biopsy rate on repeat targeted biopsy and assumption that the improved targeting technique would confer a 15% increase in CDR. Evaluation of clinically significant cancer on standard biopsy was defined by previously published Epstein criteria [13,18].

Data analysis was completed using SPSS v.15.0 software (IBM Corp., Armonk, NY, USA). Categoric variable comparisons were performed using the chi-square or Fisher exact test, and continuous variables were evaluated with the Student t test or Mann-Whitney test. Biopsy yield was assessed by McNemar test. Multivariate analysis was performed using binomial logistic regression. A p value <0.05 was used to define significant results. Targeted biopsy results were reported in accordance with the Standards of Reporting for MRI-targeted Biopsy Studies (START) recommendations where possible [19].

3. Results

3.1. Study population

The clinical characteristics for these groups are detailed in Table 1. Among 125 men enrolled, 67 (54%) had had no prior prostate biopsy (group 1), 34 (27%) had had a prior negative prostate biopsy (group 2), and 24 (19%) had been previously diagnosed with low-risk cancer on active surveillance (group 3).

The study targeted 172 separate mSR, with an overall median suspicion score of 3 [2.0–4.0]. Single targets were present in 76 patients (60.8%), while 48 men (38.4%) had two separate mSR. A total of 93 (54.1%) mSR were targeted in group 1, 49 (28.5%) in group 2, and 30 (17.4%) in group 3.

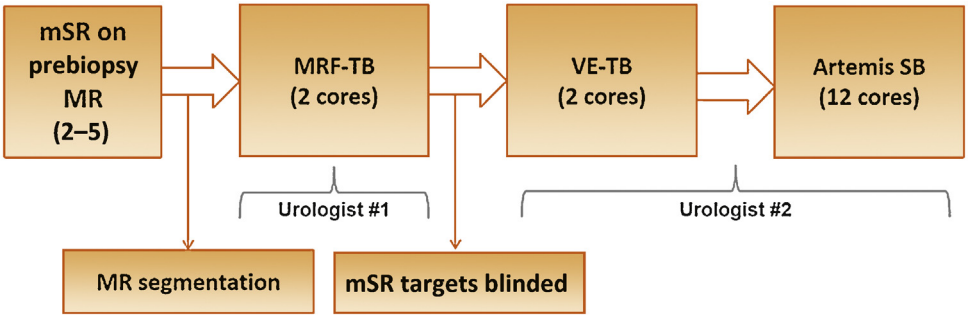

Fig. 3 – Study work flow.
mSR = magnetic resonance imaging–suspicious regions; MR = magnetic resonance; MRF-TB = magnetic resonance imaging–ultrasound fusion targeted biopsy; VE-TB = visually estimated targeted biopsy; SB = standard biopsy.

Table 1 – Patient characteristics

	Entire cohort ($n = 125$)	Group 1: biopsy naïve ($n = 67$ [54%])	Group 2: prior negative biopsy ($n = 34$ [27%])	Group 3: active surveillance ($n = 24$ [19%])	p
Age, yr (range)	65 (56.3–71.0)	65 (56.0–70.0)	63 (59.0–70.5)	68.5 (55.0–71.0)	0.676
PSA, ng/ml (range)	5.1 (3.50–7.31)	5.1 (3.40–6.90)	5.6 (4.0–9.60)	4.3 (2.40–6.87)	0.024
Prostate volume, MRI, median, ml (range)	46 (31.0–62.5)	40.5 (29.25–61.00)	51 (39.00–63.50)	48 (30.25–72.00)	0.346

PSA = prostate-specific antigen; MRI = magnetic resonance imaging.

Please cite this article in press as: Wysock JS, et al. A Prospective, Blinded Comparison of Magnetic Resonance (MR) Imaging–Ultrasound Fusion and Visual Estimation in the Performance of MR-targeted Prostate Biopsy: The PROFUS Trial. Eur Urol (2014), http://dx.doi.org/10.1016/j.eururo.2013.10.048

Table 2 – Characteristics of magnetic resonance imaging–suspicious regions

	Entire cohort (n = 125)	Group 1: biopsy naïve (n = 67 [54%])	Group 2: prior negative (n = 34 [27%])	Group 3: active surveillance (n = 24 [19%])	p
mSR, total (%)	172	93 (54.1)	49 (28.5)	30 (17.4)	–
mSR score, median (range)	3 (2.0–4.0)	3 (2.0–4.0)	3 (2.0–4.0)	3 (2.0–3.0)	0.999
Location					
Posterior, no. (%)	140 (81.4)	85 (91.4)	32 (65.3)	23 (76.7)	0.765
	32 (18.6)	8 (8.6)	17 (34.7)	7 (23.3)	0.873
Prostate region					
Base, no. (%)	45 (26.2)	23 (24.7)	13 (26.5)	9 (30.0)	0.652
Mid, no. (%)	81 (47.1)	47 (50.6)	22 (44.9)	12 (40.0)	0.788
Apex, no. (%)	46 (26.7)	23 (24.7)	14 (28.6)	9 (30.0)	0.823
Cross-sectional area, cm^2, median (range)	0.48 (0.28–0.96)	0.5 (0.30–1.00)	0.48 (0.280–1.096)	0.36 (0.210–0.783)	0.210
Diameter, mm, median (range)	9 (7–13)	9 (7–13)	7 (6–15)	8 (6–13)	0.489
Very high-suspicion mSR (5 of 5), no. (%)	21 (12.2)	17 (18.3)	3 (6.1)	1 (3.3)	–
Cross-sectional area, cm^2, median (range)	1.2 (1.00–2.40)	1.1 (0.86–1.76)	4.0 (2.32–4.0)	2.52	0.021
Diameter, mm, median (range)	14 (11.5–21)	14 (11.5–16.5)	23 (2–23)	24	0.269
High-suspicion mSR (4 of 5), no. (%)	38 (22.1)	23 (24.7)	12 (24.5)	3 (10)	–
Cross-sectional area, cm^2, median (range)	0.58 (0.331–0.955)	0.50 (0.302–0.648)	0.96 (0.430–2.573)	0.42 (0.302–0.420)	0.076
Diameter, mm, median (range)	11 (7.75–16.25)	9 (7–13)	17.5 (8–22)	9 (8–9)	0.151
Equivocal suspicion mSR (3 of 5), no. (%)	48 (27.9)	23 (24.7)	12 (24.5)	13 (43.3)	–
Cross-sectional area, cm^2, median (range)	0.42 (0.267–0.689)	0.41 (0.266–0.729)	0.47 (0.391–0.624)	0.38 (0.29–0.920)	0.544
Diameter, mm, median (range)	8 (7–11)	8 (8–11)	7.5 (7–9)	8 (6.13)	0.660
Low-suspicion mSR (2 of 5), no. (%)	65 (37.8)	30 (32.3)	22 (44.9)	13 (43.3)	–
Cross-sectional area, cm^2, median (range)	0.36 (0.202–0.811)	0.43 (0.265–0.904)	0.35 (0.167–0.653)	0.28 (0.202–0.709)	0.537
Diameter, mm, median (range)	7 (5–10)	8 (5–10.25)	6.5 (3.75–9.5)	7 (5.5–11)	0.636
Area p	<0.001	<0.0001	0.005	0.194	–
Diameter p	<0.001	0.002	0.002	0.34	–

mSR = magnetic resonance imaging–suspicious regions.

The distribution of mSR and median suspicion score did not differ among these groups. The distribution of suspicion score for mSR detected within the entire cohort and each individual group are presented in Table 2. The likelihood of a high suspicion (4–5/5) mSR was 40 of 93 (43%), 15 of 49 (30.6%), and 4 of 30 (13.3%) among groups 1, 2, and 3, respectively. No technical failures or adverse events occurred during the study period.

3.2. Targeted biopsy outcomes: magnetic resonance imaging–ultrasound fusion versus visual estimation

The CDR among 172 targeted mSR on MRF-TB was 55 (32.0%) compared with 46 (26.7%) using VE-TB (p = 0.1374; Table 3). MRF-TB detected 35 (20.3%) Gleason sum ≥7 compared with 26 (15.1%) by VE-TB (p = 0.0523). Overall CDR per patient was 45 (36.0%) and 40 (32.0%), and Gleason sum ≥7 CDR was 29 (23.2%) and 24 (19.2%) by MRF-TB and VE-TB, respectively (p = 0.3588, p = 0.2673). The overall CDR for mSR 3–5 per target was 45 (42.1%) versus 41 (38.3%) and per patient was 41 (46.6%) versus 39 (44.3%) for MRF-TB and VE-TB, respectively (p = 0.3743, p = 0.3168).

Because negative targeted biopsy represents possible false-positive mSR or a missed target, we evaluated the frequency of an informative biopsy defined as any pathologic diagnosis other than benign tissue (Table 4). Overall, MRF-TB was informative in 77 targets compared with 60 targets by VE-TB (p = 0.0104).

False negatives, defined as positive on one targeting method and negative on another, were observed for both MRF-TB and VE-TB (Table 5). By MRF-TB, 5.8% were falsely negative, and 2.3% were falsely classified as Gleason sum <7. Conversely, by VE-TB, 7.6% were falsely negative and 4.1% were falsely classified as Gleason sum <7.

3.3. Targeted biopsy outcomes: targeted biopsy compared with Artemis 12-core biopsy

Table 6 displays the comparison of the pooled targeted biopsy to standard biopsy results in group 1. Standard biopsy demonstrated higher overall CDR (37 [55.2%] vs 27 [40.3%]; p = 0.0094) and more Gleason 6 disease (15 [22.4%] vs 5 [7.5%]; p = 0.0044) but detected an equivalent number of Gleason sum ≥7 (22 [32.8%] vs 22 [32.8%]; p = 0.6831). No Gleason sum ≥7 disease detected by standard biopsy were missed on targeted biopsy, but two Gleason sum ≥7 instances were classified as Gleason 6. Biopsy yield decreased as the degree of mSR suspicion decreased with CDR of Gleason sum ≥7 disease, approaching zero in the low-suspicion group.

Using Epstein criteria, standard biopsy detected clinical significant cancer in 28 men (41.8%), 22 (78.6%) Gleason sum ≥7 and 6 (21.4%) by core number and cancer length. Of the 22 cases of Gleason sum ≥7 disease on standard biopsy, targeted biopsy detected 19 (86.4%) and classified 3 (13.6%) as Gleason 6 disease. Of the six CS Gleason 6 cases detected on standard biopsy, targeted biopsy classified two (33.3%)

Please cite this article in press as: Wysock JS, et al. A Prospective, Blinded Comparison of Magnetic Resonance (MR) Imaging–Ultrasound Fusion and Visual Estimation in the Performance of MR-targeted Prostate Biopsy: The PROFUS Trial. Eur Urol (2014), http://dx.doi.org/10.1016/j.eururo.2013.10.048

Table 3 – Targeted biopsy results

mSR (targets, patients)	Entire cohort				Group 1: biopsy naïve				Group 2: prior negative				Group 3: active surveillance			
	MRF-TB		VE-TB		MRF-TB		VE-TB		MRF-TB		VE-TB		MRF-TB		VE-TB	
Entire cohort (172, 125)																
Cancer																
Target	55	32.0%	46	26.7%	30	32.3%	25	26.9%	13	26.5%	9	18.4%	12	40.0%	12	40.0%
Patient	45	36.0%	40	32.0%	24	35.8%	23	34.3%	10	29.4%	8	23.5%	11	45.8%	9	37.5%
Gleason sum ≥7																
Target	35	20.3%	26	15.1%	23	24.7%	19	20.4%	8	16.3%	6	12.2%	4	13.3%	1	3.3%
Patient	29	23.2%	24	19.2%	19	28.4%	18	26.9%	7	20.6%	5	14.7%	3	12.5%	1	4.2%
Very high suspicion (21, 19)																
Cancer																
Target	18	85.7%	16	76.2%	14	82.4%	13	76.5%	3	100.0%	2	66.7%	1	100.0%	1	100.0%
Patient	17	89.5%	15	78.9%	14	87.5%	13	81.3%	2	100.0%	1	50.0%	1	100.0%	1	100.0%
Gleason sum ≥7																
Target	17	81.0%	13	61.9%	13	76.5%	11	64.7%	3	100.0%	2	66.7%	1	100.0%	0	0.0%
Patient	16	84.2%	12	63.2%	13	81.3%	11	68.8%	2	100.0%	1	50.0%	1	100.0%	0	0.0%
High suspicion (38, 32)																
Cancer																
Target	16	42.1%	16	42.1%	8	34.8%	8	34.8%	6	50.0%	6	50.0%	2	66.7%	2	66.7%
Patient	13	40.6%	15	46.9%	5	29.4%	7	41.2%	6	50.0%	6	50.0%	2	66.7%	2	66.7%
Gleason sum ≥7																
Target	12	31.6%	11	28.9%	7	30.4%	6	26.1%	5	41.7%	4	33.3%	0	0.0%	1	33.3%
Patient	9	28.1%	11	14.3%	4	23.5%	6	35.3%	5	41.7%	4	33.3%	0	0.0%	1	33.3%
Equivocal suspicion (48, 32)																
Cancer																
Target	11	22.9%	10	20.8%	3	12.0%	3	12.0%	1	9.1%	1	9.1%	7	53.8%	6	46.2%
Patient	11	29.7%	8	21.6%	3	16.7%	3	16.7%	1	10.0%	1	10.0%	7	70.0%	4	40.0%
Gleason sum ≥7																
Target	4	8.3%	1	2.1%	1	4.0%	1	4.0%	0	0.0%	0	0.0%	3	23.1%	0	0.0%
Patient	3	8.1%	1	2.7%	1	5.6%	1	5.6%	0	0.0%	0	0.0%	2	20.0%	0	0.0%
Low suspicion (65, 37)																
Cancer																
Target	10	15.4%	4	6.2%	5	17.2%	1	3.4%	3	13.0%	0	0.0%	2	15.4%	3	23.1%
Patient	4	10.8%	1	2.7%	2	11.8%	0	0.0%	1	10.0%	0	0.0%	1	10.0%	1	10.0%
Gleason sum ≥7																
Target	2	3.1%	1	1.5%	2	6.9%	1	3.4%	0	0.0%	0	0.0%	0	0.0%	0	0.0%
Patient	1	2.7%	0	0.0%	1	5.9%	0	0.0%	0	0.0%	0	0.0%	0	0.0%	0	0.0%

mSR = magnetic resonance imaging–suspicious regions; MRF-TB = magnetic resonance imaging–ultrasound fusion targeted biopsy; VE-TB = visually estimated targeted biopsy.

as Gleason sum ≥7, two (33.3%) as Gleason 6 disease, and two (33.3%) as no cancer. Overall, targeted biopsy diagnosed 21 (75.0%) clinically significant cases detected on standard biopsy by Epstein criteria.

Sampling efficiency, as measured by mean length of cancer per positive core per patient, mean percent of cancer per positive biopsy core per patient, and number of cores positive per cores sampled, was significantly greater in the

Table 4 – Biopsy information by level of magnetic resonance imaging–suspicious regions

Target results	All mSR		Very high suspicion		High suspicion		Equivocal suspicion		Low suspicion	
	MRF-TB	VE-TB	MRF-TB	VE-TB	MRF-TB	VE-TB	MRF-TB	VE-TB	MRF-TB	VE-TB
Benign, no.	95	112	0	3	15	18	33	34	47	57
Inflammation, no.	17	12	3	2	6	4	2	2	6	4
HGPIN, no.	2	0	0	0	1	0	1	0	0	0
ASAP, no.	3	2	0	0	0	0	1	2	0	0
3 + 3, no.	20	20	1	3	4	5	7	9	8	3
3 + 4, no.	19	14	7	4	6	8	4	1	2	1
4 + 3, no.	2	2	0	1	2	1	0	0	0	0
4 + 4, no.	6	7	5	6	1	1	0	0	0	0
3 + 5, no.	1	0	1	0	0	0	0	0	0	0
4 + 5, no.	7	3	4	2	3	1	0	0	0	0
Total non-benign	77*	60	21	18	23	20	15	14	16	8

mSR = magnetic resonance imaging–suspicious regions; MRF-TB = magnetic resonance imaging–ultrasound fusion targeted biopsy; VE-TB = visually estimated targeted biopsy; HGPIN = high-grade prostatic intraepithelial neoplasia; ASAP = atypical small acinar proliferation of prostate.
* $p = 0.0104$.

Please cite this article in press as: Wysock JS, et al. A Prospective, Blinded Comparison of Magnetic Resonance (MR) Imaging–Ultrasound Fusion and Visual Estimation in the Performance of MR-targeted Prostate Biopsy: The PROFUS Trial. Eur Urol (2014), http://dx.doi.org/10.1016/j.eururo.2013.10.048

Table 5 – Cancer detection rate by targeted biopsy technique

	MRF-TB			
	Gleason sum ≥7, no. (%)	Gleason 6, no. (%)	No cancer, no. (%)	Total, no. (%)
VE-TB				
Gleason sum ≥7	22 (12.8)	0 (0)	4 (2.3)	26 (15.1)
Gleason 6	7 (4.1)	7 (4.1)	6 (3.5)	20 (11.6)
No cancer	6 (3.5)	13 (7.6)	107 (62.2)	126 (73.3)
Total	35 (20.3)	20 (11.6)	117 (68.0)	172

MRF-TB = magnetic resonance imaging–ultrasound fusion targeted biopsy; VE-TB = visually estimated targeted biopsy.

Table 6 – Comparison of cancer detection rate between targeted biopsy and 12-core biopsy in biopsy-naïve patients (group 1)

	Targeted biopsy (MRF-TB and VE-TB)			
	Gleason sum ≥7, no. (%)	Gleason 6, no. (%)	No cancer, no. (%)	Total, no. (%)
12-core biopsy				
Gleason sum ≥7	19 (28.4)	3 (4.5)	0 (0)	22 (32.8)
Gleason 6	2 (3.0)	1 (1.5)	12 (17.9)	15 (22.4)
No cancer	1 (1.5)	1 (1.5)	28 (26.9)	30 (44.8)
Total	22 (32.8)	5 (7.5)	40 (59.7)	67

MRF-TB = magnetic resonance imaging–ultrasound fusion targeted biopsy; VE-TB = visually estimated targeted biopsy.

Table 7 – Cancer length, percentage of cancer, and number of positive cores by biopsy technique

	MRF-TB		VE-TB		Targeted biopsy (MRF-TB and VE-TB)		Standard biopsy	
	Mean	SD	Mean	SD	Mean	SD	Mean	SD
Cancer core length (mm) per positive core, per patient								
All cancer	4.69	3.31	5.12	4.11	3.75*	3.16	2.86*	2.41
Gleason sum ≥7	5.74	3.40	6.75	4.10	4.95*	3.32	3.69*	2.50
Percentage of cancer core length								
All cancer	45.62	24.89	43.18	27.90	34.25*	23.45	26.12*	19.41
Gleason sum ≥7	53.00	22.04	53.56	25.69	43.11*	22.20	33.34*	17.45
	Total	%	Total	%	Total	%	Total	%
No. of positive cores								
All cancer	55	16.0	45	13.1	65*	9.4	86*	5.7
Gleason sum ≥7	35	10.2	26	7.6	39	5.7	48	3.2

MRF-TB = magnetic resonance imaging–ultrasound fusion targeted biopsy; VE-TB = visually estimated targeted biopsy.
* $p < 0.05$.

targeted biopsy cases than in the standard biopsy cases (Table 7). No significant differences were seen in these parameters between targeting techniques.

3.4. *Multivariate analysis of predictors of positive magnetic resonance imaging–ultrasound fusion targeted biopsy*

On multivariate analysis, decreased mSR diameter was significantly associated with cancer detection using MRF-TB (Table 8).

3.5. *Multivariate analysis of predictors of positive targeted biopsy*

Smaller MR prostate volume and increasing mSR suspicion score predicted increased CDR on targeted biopsy (Table 9).

4. Discussion

Much of the current dilemma regarding prostate cancer (PCa) screening, detection, and appropriate treatment can be attributed to the use of random sampling methods for prostate biopsy [20–22]. Standard biopsy relies on sampling efficiency for cancer detection, which intrinsically risks the consequences of sampling error: undersampling, oversampling, and inaccurate risk stratification [23]. Despite increasing evidence to support a benefit for MR-TB in PCa detection, the optimal method for MR-TB is unknown [15,24].

Several recent studies have evaluated the outcome of MRF-TB [1,2,25,26]. Regardless of coregistration or biopsy method, the study results are generally similar. MRF-TB demonstrates lower overall CDR than standard biopsy but

Please cite this article in press as: Wysock JS, et al. A Prospective, Blinded Comparison of Magnetic Resonance (MR) Imaging–Ultrasound Fusion and Visual Estimation in the Performance of MR-targeted Prostate Biopsy: The PROFUS Trial. Eur Urol (2014), http://dx.doi.org/10.1016/j.eururo.2013.10.048

Table 8 – Multivariate analysis of positive magnetic resonance imaging–ultrasound fusion targeted biopsy and negative visually estimated targeted biopsy

Variable	Univariate analysis			Multivariate analysis		
	OR	95% CI	*p*	OR	95% CI	*p*
Age, yr	1.01	0.96–10.7	0.704	1.05	0.98–1.14	0.181
PSA, ng/ml	0.96	0.85–1.08	0.509	0.91	0.78–1.08	0.280
Prostate volume, MRI, ml	0.99	0.96–1.00	0.168	0.98	0.96–1.00	0.187
mSR suspicion score:						
2	Ref	–	–	Ref	–	–
3	0.83	0.25–2.71	0.756	1.55	0.39–6.10	0.534
4	0.84	0.24–2.99	0.786	1.45	0.32–6.55	0.630
5	0.75	0.15–3.84	0.73	0.64	0.06–7.11	0.713
mSR diameter	0.89	0.80–1.00	0.048	0.83	0.73–0.95	0.005
mSR cross-sectional area	1.15	0.66–2.00	0.631	2.27	0.81–6.38	0.120
mSR location						
Posterior	Ref	–	–	Ref	–	–
Anterior	2.99	1.07–8.33	0.037	3.84	1.00–14.72	0.050
Operator experience with VE-TB						
Inexperienced	Ref	–	–	Ref	–	–
Experienced	0.76	0.29–.197	0.572	0.64	0.19–2.13	0.467

OR = odds ratio; CI = confidence interval; PSA = prostate-specific antigen, MRI = magnetic resonance imaging; mSR = magnetic resonance imaging–suspicious regions; VE-TB = visually estimated targeted biopsy.

Table 9 – Multivariate analysis of predictors of positive targeted biopsy (magnetic resonance imaging–ultrasound fusion targeted biopsy and visually estimated targeted biopsy) in group 1

Variable	Univariate analysis			Multivariate analysis		
	OR	95% CI	*p*	OR	95% CI	*p*
Age, yr	1.07	1.03–1.11	0.002	1.05	1.00–1.11	0.072
PSA, ng/ml	1.14	1.05–1.23	0.002	1.11	1.00–1.24	0.051
Prostate volume, MRI, ml	0.99	0.98–1.00	0.171	0.98	0.97–1.00	0.021
mSR suspicion score						
2	Ref	–	–	Ref	–	–
3	2.01	0.84–4.81	0.118	2.69	1.00–7.26	0.500
4	4.91	2.01–11.99	<0.001	5.82	2.04–16.57	0.001
5	26.5	6.71–104.65	<0.001	23.24	4.24–127.42	<0.001
mSR diameter	1.07	1.02–1.13	0.013	0.91	0.81–1.02	0.113
mSR cross-sectional area	2.441	1.50–3.97	<0.001	2.03	0.77–5.32	0.151
mSR location						
Posterior	Ref	–	–	Ref	–	–
Anterior	2.99	1.36–6.57	0.007	2.4	0.81–7.12	0.116
Operator experience with VE-TB						
Inexperienced	Ref	–	–	Ref	–	–
Experienced	1.53	0.82–2.85	0.183	1.19	0.50–2.86	0.698

OR = odds ratio; CI = confidence interval; PSA = prostate-specific antigen, MRI = magnetic resonance imaging; mSR = magnetic resonance imaging–suspicious regions; Ref = reference; VE-TB = visually estimated targeted biopsy.

more frequently demonstrates higher-grade cancers. In addition, positive cores are more frequently observed with MRF-TB than with standard biopsy, and positive cores carry a greater length of cancer. These findings are similar to previously reported studies of VE-TB, suggesting that MRF-TB has equivalent outcomes and may avoid issues of operator experience with MR interpretation and visual targeting.

Puech et al. compared an electromagnetic MRI-US fusion biopsy system (MyLab Navigator, Esoate, Genoa, Italy) to VE-TB in 95 men without prior biopsy in a multicenter prospective trial design [25]. Despite the prospective nature of the study, only 68 of 95 (71.6%) men underwent both MRI-US fusion and VE-TB, thus limiting the power of the study. The authors demonstrated no difference in cancer detection between techniques. These findings may be attributed in part to the considerable experience level of the operators in VE-TB, as the authors suggest, but is more likely the result of inadequate patient numbers.

Although our study was designed to answer the same question as Puech et al., several critical distinctions can be made. First, we chose to include men who had had previous negative and positive biopsy. In doing so, we focused our outcome on a lesion-based analysis rather than overall cancer detection. Second, MRF-TB was performed by a single, separate operator prior to VE-TB and standard

Please cite this article in press as: Wysock JS, et al. A Prospective, Blinded Comparison of Magnetic Resonance (MR) Imaging–Ultrasound Fusion and Visual Estimation in the Performance of MR-targeted Prostate Biopsy: The PROFUS Trial. Eur Urol (2014), http://dx.doi.org/10.1016/j.eururo.2013.10.048

biopsy. In doing so, the accuracy of MRF-TB improves because of minimization of patient movement and gland distorting resulting from hemorrhage or needle insertion.

Our study demonstrated no difference in CDR between MRF-TB and VE-TB, but a trend toward improved CDR was observed overall and in all subsets, suggesting that our study may have benefited from a larger sample size.

Potential benefits for MRF-TB were also observed. The presence of a nonmalignant pathologic abnormality on targeted biopsy may indicate that the target was hit and raises the likelihood of a true negative. In this study, an informative diagnosis was more frequently identified on MRF-TB than on VE-TB (77 vs 60, $p = 0.0104$). Our observations of improved targeting using MRF-TB occurred despite significant experience with VE-TB over the past 5 yr, suggesting that a greater magnitude of benefit and improved CDR may be noted in centers with little or no experience in VE-TB.

Although this study was not powered to compare targeted biopsy and standard biopsy, several observations can be made from our subset analyses. The likelihood of cancer varied by suspicion score, as shown in other studies, but for a given suspicion score, the CDR varied by indication for biopsy. Men with known cancer carried a higher CDR when targeting equivocal or high-suspicion lesions compared with biopsy-naïve men. This observation suggests that cancer risk, as defined by level of suspicion, needs to be adjusted with the prevalence of cancer in the biopsy cohort. Further larger studies integrating MRI within risk models are warranted in this regard.

The CDR was significantly greater with standard biopsy than with targeted biopsy among biopsy-naïve men, but targeted biopsy identified all cancers with Gleason sum $\geq$7. The fact that a small number of Gleason sum $\geq$7 cancers were classified as Gleason sum 6 on MRF-TB suggests that improvements in targeting are warranted. Several factors may influence sampling efficiency on targeted biopsy, including core number, lesion size, suspicion scale, operator, and method of targeting. Although suspicion score correlated with CDR, low-suspicion targets tended to be smaller, indicating that modified biopsy and targeting technique may improve CDR further.

Similar to previous reports, out study demonstrates that more cancer is found on a per-lesion and per-core basis with targeted biopsy than standard biopsy but did not differ between targeting methods [1,13,25,26]. This observation is true across cohorts and suggests that targeted biopsy will ultimately provide greater concordance with final pathology.

A unique aspect of this study is that it allows for the comparison of three biopsy techniques in an individual patient. Multivariate analysis regarding predictors of both MRF-TB and targeted biopsy suggest that the most influential factors for cancer detection by MRF-TB and targeted biopsy were smaller lesion diameter and lesion suspicion score and MR volume, respectively. These findings imply that software coregistration provides the greatest impact when targeting smaller targets that may be difficult to identify using VE-TB. Overall, the CDR on targeted biopsy appears to correlate with increasing suspicion of mSR, with further improvement occurring in smaller glands, likely because of decreased sampling error and needle deflection.

Several additional potential limitations of our study are worth mentioning. Limiting target sampling to two cores increases the risk of missed targets, particularly when the targets are small. Because the patients were not ultimately evaluated with prostatectomy, the significance of negative biopsy findings remains unclear. The study was performed in a setting of significant clinical experience with the implementation of mpMRI and VE-TB, which may bias the study in favor of VE-TB. Finally, the CDR with Artemis-directed standard biopsy in biopsy-naïve men was quite high (55.2%) relative to existing literature. Whether the Artemis standard biopsy provides a higher CDR than conventional standard biopsy is unknown, and its use may have influenced the comparative outcomes of standard biopsy and targeted biopsy.

5. Conclusions

In this study, MRF-TB was more often histologically informative than VE-TB, and although it did not provide a higher CDR, a trend toward an improved CDR with MRF-TB was noted in all subsets, suggesting a need for a larger sample size. Targeting was improved by MRF among smaller lesions. A software-based coregistration tool would likely assist the community adoption of MRI-TB, especially in centers that have limited experience with visual targeting. This study prompts additional work into the use of targeted biopsy in distinct clinical scenarios. Among men with no prior biopsy, low levels of suspicion predict a low likelihood of significant cancer, thus offering a potential avenue for reduction of overdetection.

Author contributions: Samir S. Taneja had full access to all the data in the study and takes responsibility for the integrity of the data and the accuracy of the data analysis.

Study concept and design: Taneja, Wysock.
Acquisition of data: Taneja, Huang, Stifelman, Lepor, Deng, Melamed, Wysock.
Analysis and interpretation of data: Taneja, Rosenkrantz, Wysock.
Drafting of the manuscript: Wysock.
Critical revision of the manuscript for important intellectual content: Taneja, Rosenkrantz, Wysock.
Statistical analysis: Wysock.
Obtaining funding: None.
Administrative, technical, or material support: Wysock.
Supervision: Taneja.
Other (specify): None.

Financial disclosures: Samir S. Taneja certifies that all conflicts of interest, including specific financial interests and relationships and affiliations relevant to the subject matter or materials discussed in the manuscript (eg, employment/affiliation, grants or funding, consultancies, honoraria, stock ownership or options, expert testimony, royalties, or patents filed, received, or pending), are the following: None.

Funding/Support and role of the sponsor: None.

Please cite this article in press as: Wysock JS, et al. A Prospective, Blinded Comparison of Magnetic Resonance (MR) Imaging–Ultrasound Fusion and Visual Estimation in the Performance of MR-targeted Prostate Biopsy: The PROFUS Trial. Eur Urol (2014), http://dx.doi.org/10.1016/j.eururo.2013.10.048

References

[1] Pinto PA, Chung PH, Rastinehad AR, et al. Magnetic resonance imaging/ultrasound fusion guided prostate biopsy improves cancer detection following transrectal ultrasound biopsy and correlates with multiparametric magnetic resonance imaging. J Urol 2011; 186:1281–5.

[2] Hadaschik BA, Kuru TH, Tulea C, et al. A novel stereotactic prostate biopsy system integrating pre-interventional magnetic resonance imaging and live ultrasound fusion. J Urol 2011;186:2214–20.

[3] Hambrock T, Somford DM, Hoeks C, et al. Magnetic resonance imaging guided prostate biopsy in men with repeat negative biopsies and increased prostate specific antigen. J Urol 2010; 183:520–7.

[4] Lee SH, Chung MS, Kim JH, Oh YT, Rha KH, Chung BH. Magnetic resonance imaging targeted biopsy in men with previously negative prostate biopsy results. J Endourol 2012;26:787–91.

[5] Dickinson L, Ahmed HU, Allen C, et al. Magnetic resonance imaging for the detection, localisation, and characterisation of prostate cancer: recommendations from a European consensus meeting. Eur Urol 2011;59:477–94.

[6] Kirkham APS, Emberton M, Allen C. How good is MRI at detecting and characterising cancer within the prostate? Eur Urol 2006; 50:1163–75, discussion 1175.

[7] Hambrock T, Fütterer JJ, Huisman HJ, et al. Thirty-two-channel coil 3T magnetic resonance-guided biopsies of prostate tumor suspicious regions identified on multimodality 3T magnetic resonance imaging: technique and feasibility. Invest Radiol 2008;43:686–94.

[8] Singh AK, Krieger A, Lattouf JB, et al. Patient selection determines the prostate cancer yield of dynamic contrast-enhanced magnetic resonance imaging-guided transrectal biopsies in a closed 3-Tesla scanner. BJU Int 2008;101:181–5.

[9] Engelhard K, Hollenbach HP, Kiefer B, Winkel A, Goeb K, Engehausen D. Prostate biopsy in the supine position in a standard 1.5-T scanner under real time MR-imaging control using a MR-compatible endorectal biopsy device. Eur Radiol 2006;16:1237–43.

[10] Beyersdorff D, Winkel A, Hamm B, Lenk S, Loening SA, Taupitz M. MR imaging-guided prostate biopsy with a closed MR unit at 1.5 T: initial results. Radiology 2005;234:576–81.

[11] Roethke M, Anastasiadis AG, Lichy M, et al. MRI-guided prostate biopsy detects clinically significant cancer: analysis of a cohort of 100 patients after previous negative TRUS biopsy. World J Urol 2012;30:213–8.

[12] Sciarra A, Panebianco V, Ciccariello M, et al. Value of magnetic resonance spectroscopy imaging and dynamic contrast-enhanced imaging for detecting prostate cancer foci in men with prior negative biopsy. Clin Cancer Res 2010;16:1875–83.

[13] Haffner J, Lemaitre L, Puech P, et al. Role of magnetic resonance imaging before initial biopsy: comparison of magnetic resonance imaging-targeted and systematic biopsy for significant prostate cancer detection. BJU Int 2011;108:E171–8.

[14] Park BK, Park JW, Park SY, et al. Prospective evaluation of 3-T MRI performed before initial transrectal ultrasound-guided prostate biopsy in patients with high prostate-specific antigen and no previous biopsy. AJR Am J Roentgenol 2011;197:W876–81.

[15] Moore CM, Robertson NL, Arsanious N, et al. Image-guided prostate biopsy using magnetic resonance imaging-derived targets: a systematic review. Eur Urol 2013;63:125–40.

[16] Barentsz JO, Richenberg J, Clements R, et al., European Society of Urogenital Radiology. ESUR prostate MR guidelines 2012. Eur Radiol 2012;22:746–57.

[17] Narayanan R, Kurhanewicz J, Shinohara K, Crawford ED, Simoneau A, Suri JS. MRI-ultrasound registration for targeted prostate biopsy. Presented at: IEEE International Symposium on Biomedical Imaging: From Nano to Macro, 2009; June 28–July 1, 2009; Boston, MA, USA.

[18] Epstein JI, Walsh PC, Carmichael M, Brendler CB. Pathologic and clinical findings to predict tumor extent of non palpable (stage T1c) prostate cancer. JAMA 1994;271:368–74.

[19] Moore CM, Kasivisvanathan V, Eggener S, et al., START Consortium. Standards of reporting for MRI-targeted biopsy studies (START) of the prostate: recommendations from an international working group. Eur Urol 2013;64:544–52.

[20] Cooperberg MR, Broering JM, Kantoff PW, Carroll PR. Contemporary trends in low risk prostate cancer: risk assessment and treatment. J Urol 2007;178:S14–9.

[21] Scattoni V, Zlotta A, Montironi R, Schulman C, Rigatti P, Montorsi F. Extended and saturation prostatic biopsy in the diagnosis and characterisation of prostate cancer: a critical analysis of the literature. Eur Urol 2007;52:1309–22.

[22] Bjurlin MA, Carter HB, Schellhammer P, et al. Optimization of initial prostate biopsy in clinical practice: sampling, labeling and specimen processing. J Urol 2013;189:2039–46.

[23] Loeb S, Vellekoop A, Ahmed HU, et al. Systematic review of complications of prostate biopsy. Eur Urol 2013;64:876–92.

[24] Rosenkrantz AB, Taneja SS. Targeted prostate biopsy: opportunities and challenges in the era of multiparametric prostate magnetic resonance imaging. J Urol 2012;188:1072–3.

[25] Puech P, Rouvière O, Renard-Penna R, et al. Prostate cancer diagnosis: multiparametric MR-targeted biopsy with cognitive and transrectal US-MR fusion guidance versus systematic biopsy—prospective multicenter study. Radiology 2013;268:461–9.

[26] Sonn GA, Natarajan S, Margolis DJ, et al. Targeted biopsy in the detection of prostate cancer using an office based magnetic resonance ultrasound fusion device. J Urol 2013;189:86–91.

Please cite this article in press as: Wysock JS, et al. A Prospective, Blinded Comparison of Magnetic Resonance (MR) Imaging–Ultrasound Fusion and Visual Estimation in the Performance of MR-targeted Prostate Biopsy: The PROFUS Trial. Eur Urol (2014), http://dx.doi.org/10.1016/j.eururo.2013.10.048